Direct observation of scattering contributions in X-ray attenuation measurements, and evidence for Rayleigh scattering from copper samples rather than thermal-diffuse or Bragg–Laue scattering

C.T. Chantler[a,*], C.Q. Tran[a], D. Paterson[a], Z. Barnea[a], D.J. Cookson[b,c]

[a] *School of Physics, University of Melbourne, Parkville Vic. 3010, Australia*
[b] *Australian Nuclear Science & Technology Organisation, Private Mail Bag 1, Menai, NSW 2234, Australia*
[c] *Chem-Mat-CARS-CAT (Sector 15, Bldg 434D), Argonne National Laboratory, 9700 S, Cass Avenue, Argonne, IL 60439, USA*

Abstract

High-precision attenuation measurements can now lead to a direct assessment of scattering models in the X-ray regime. This is true not just at high energies but even when scattering cross-sections typically lie below 0.1% of the photoelectric absorption cross-section. This allows model-independent results to be obtained in these attenuation experiments for the first time. © 2001 Elsevier Science Ltd. All rights reserved.

Keywords: Attenuation coefficients; X-ray scattering; Atomic form factors

The complex form factor and the interaction cross-sections are key parameters specifying a wide range of physical properties of materials: refractive indices, scattering and attenuation coefficients, diffraction profiles, and electronic wave function distributions. Even though applications using these properties are well established, experiment and theory have not converged for virtually any elements in any energy regions (Chantler, 1995; Saloman et al., 1988; Henke et al., 1993; Creagh and McAuley, 1995). Typical experimental precisions lie at the 1–5% level, while typical accuracy is 5–10%. Major issues limiting earlier measurements at the 1–10% level included thickness profilometry and determination, monochromation and energy calibration, detector non-linearity, statistical precision and also harmonic contamination and scattering uncertainty (Chantler et al., 1999; Creagh and Hubbell, 1987). This applies even to a direct comparison of recent experimental data for the most carefully investigated elements

such as copper, for central X-ray energies (Wang et al., 1992; Kiran Kumar et al., 1996).

Scattering cross-sections in these experimental studies have been obtained from purely theoretical predictions based on the type of process expected from the material in question. However, the main alternatives vary by some orders of magnitude, so any non-ideal material will yield a poor experimental accuracy using any of these assumptions. Hence the lack of information on the scattering mechanism and the scattering coefficient has been a major limitation in earlier experiments.

The total photon interaction cross-section for a non-crystalline material (in which atoms can be approximated as isolated and independent particles) is given by

$$\sigma_{TOT} = \tau_{pe} + \sigma_R + \sigma_C + \kappa_n + \kappa_e + \sigma_{p.n.},$$

where τ_{pe} is the photoelectric cross-section, σ_R is the Rayleigh (coherent) scattering cross-section, σ_C is the Compton (incoherent) scattering cross-section, κ_n is the pair production cross-section in the nuclear field, κ_e is the pair production cross-section in the atomic electric field, and $\sigma_{p.n.}$ is the photonuclear cross-section. At moderate X-ray energies, the last three cross-sections may be neglected. In a crystalline material, there will be

*Corresponding author. Fax: +61-3-9347-4783.
E-mail addresses: chantler@ph.unimelb.edu.au (C.T. Chantler).

strong scattered peaks at certain orientations between the crystal and the incident beam. Away from those Bragg–Laue reflection orientations, there will be scattering contributions arising from small deviations in the periodic crystalline structure (diffuse scattering) and from thermal vibrations of the atoms (thermal scattering) σ_{TDS}. The total photon interaction cross-section, then, becomes

$$\sigma_{TOT} = \tau_{pe} + \sigma_{TDS} + \sigma_C.$$

Although the angular dependence of scattering can be observed using high-efficiency detectors with a high-flux synchrotron source, calibration and direct detection as part of an attenuation measurement is very difficult, due to the dominance of photoelectric scattering at low energies. This is a major challenge in the field of atomic form factors in both theory and experiment.

This paper discusses a key technical issue in our recent precision measurement of attenuation coefficients for copper (8.84–20 keV) and silicon (5–20 keV). In this experiment, the final limiting precision is reduced to 0.01–0.02%, hence allowing investigation of small systematic contributions to the signal. Because each systematic effect has a different signature, we are able to isolate contributing residual contributions.

In our experiment, we scanned a translational sample stage normal to the X-ray beam and measured the attenuation of the sample with environment (at a number of sample positions) and of the environment alone (at 'blank' positions, or with the sample out of beam). For the attenuation measurement, the attenuated signal is normalised by a matched upstream monitor, corrected for the offset noise in the detector, and any contribution from the environment is eliminated by normalising to the results for the 'blank' settings.

The upstream signal increased when a sample was inserted. Because of our low noise level and high statistical precision, this corresponded to a 3–10 standard deviation effect, repeated some 100 times across the energy range for the copper measurements.

Several possible systematic sources of error were investigated. We had observed positive and negative correlations of the detector signals due to the counting chain, but this has a completely different signature (Chantler et al., 2000). However, a positive or negative correlation in the amplifier signal due to faulty (unstable) power supplies could produce effects of a similar magnitude and must be considered.

If an amplifier correlation were to be positive, then a decrease in the downstream signal (from the insertion of a sample in the beam) would yield a decrease in the upstream signal—opposite of what we observed. If the correlation were to be negative, then insertion of a thicker absorber would yield a higher signal in the upstream monitor, as observed. This imputed source of error would also give an increase in the monitor signal as

the beam current dropped with time through a series of measurements. Tests over a 12-h period would then show non-linear detector responses as the incident flux varied by a factor of 2. However, our linearity tests, repeated every 5 min over several days, demonstrated extremely high linearity, down to the 0.03% level. Hence these sources of error were negligible in our experiment compared to the signal level for back-scattering of 0.05–0.25% of the monitor reading.

Another possibility is the presence of Bragg–Laue peaks from copper crystal planes. Although the copper samples are rolled and expected to consist of highly mosaic crystallites, there could be sufficient statistical orientation to produce alignment with a Bragg plane. If this occurred and the reflected beam did not return to the detector, then intensity would be removed from the beam and the sample would appear more attenuating than expected.

Bragg reflection off a single large grain, however, could only happen at specific incident wavelengths and samples. This would create discontinuities in the attenuation versus energy curve, which were not observed to below the 0.2% level. The possibility of a well-aligned Bragg back-reflection increasing the count rate of the upstream monitor detector was eliminated by using three samples for each energy. This back-reflection is ruled out at about the 0.02% level. Hence no Bragg–Laue planes reflect across the range of energies. Rayleigh scattering (isolated atom or ideally mosaic crystal diffraction) or thermal-diffuse scattering must be dominant.

The contribution to the monitor signal from the back-scattering component was directly observed by comparing monitor readings with and without an absorber. The dependence of this back-scattering signal upon energy is given in Fig. 1. The scattering component has a smoothly increasing signal with energy above the absorption edge. A significant fraction of this back-scattered signal is due to fluorescence—the emission of lower energy characteristic radiation after absorption of the full photon energy. This is similar to incoherent scattering but has a much larger amplitude (at low energies) and is properly represented as two independent steps rather than a single scattering event. The remainder of the signal is due to Rayleigh scattering, although there is the possibility of thermal diffuse scattering (TDS) instead. However, the amplitude for TDS is an order of magnitude less than that for Rayleigh scattering. TDS is consistent with the very low signal of less than 0.01% observed in another experiment with silicon absorbers, but is not consistent with the signal observed here. Hence, it appears that a combination of Rayleigh scattering and fluorescence explain the magnitude and angular symmetry of the signal. Fig. 2 indicates the results of modelling in our geometry.
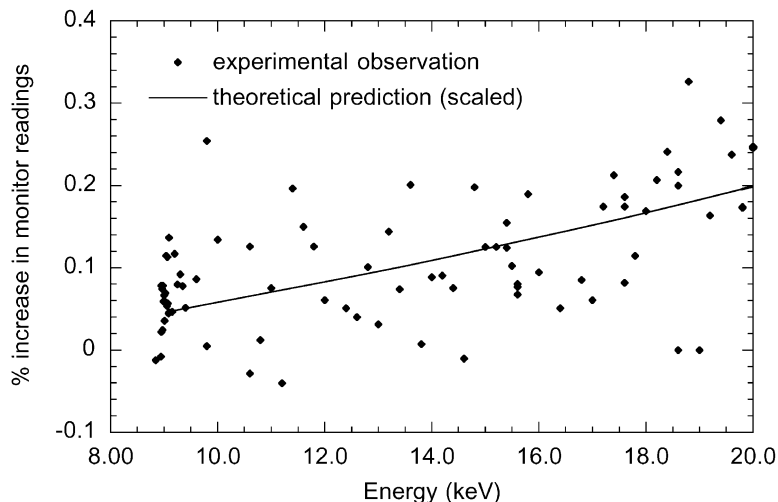
Fig. 1. Percentage increase in the upstream monitor reading upon insertion of an absorber downstream. The 0.05–0.2% model-based prediction based on Rayleigh scattering is a smooth fit to the data, with a standard deviation of 0.05%. The experimental observations represent a series of foil thicknesses and must have a significant scatter as observed.
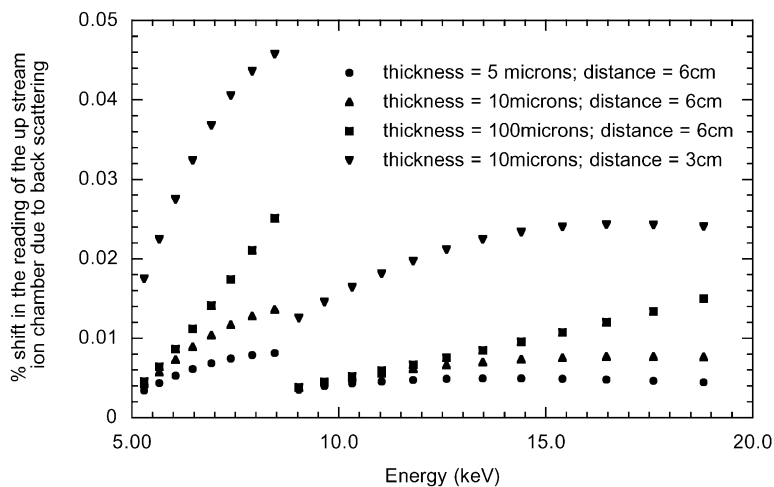

Fig. 2. A 0.01–0.05% additional signal on the upstream monitor is predicted from modelling based on Rayleigh scattering cross-sections alone. The dependence of the signal upon energy is in very good agreement with that observed, which is primarily a confirmation of the relative importance of absorption compared to scattering as a function of energy. The predicted signal is less than that observed, implying the presence of significant fluorescence above the absorption edge, which has been verified by an observation of the energies of the scattered photons.

Although the back-scattering from Rayleigh scattering and fluorescence is large, the effect of either on the final attenuation measurements is negligible because of the forward-backwards symmetry (Fig. 3). In other words, although the upstream signal increases by e.g. 0.1% upon insertion of an absorber, modelling of both fluorescence and Rayleigh scattering implies that the downstream signal increases by the same percentage, and hence the forward and back-scattering cancel out.

Fig. 3 also shows that this is not necessarily true for all experimental geometries. In particular, if the solid angle subtended by the two detectors from the sample source is not similar, or if the detectors are not properly matched, then this signal would not cancel. Another interesting result is that the cancellation is not exact, and a $\pm0.003-\pm0.02\%$ correction may be needed depending upon the sample thickness and the attenuation coefficient. This 'correction' is, therefore, less than 0.02% and is insignificant compared to other contributions. Indeed,
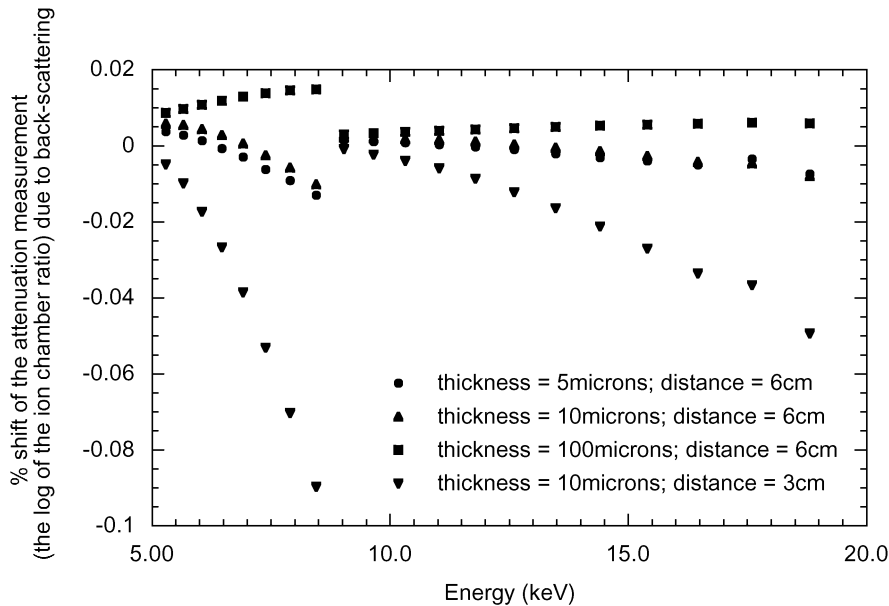
Fig. 3. A 0.01–0.05% signal is seen to have an effect of less than 0.005% on the evaluation of the attenuation coefficient if the detectors are matched and at equidistant from the absorber.

the fact that we can determine this contribution at all indicates that all other sources of error have been minimised.

References

Chantler, C.T., 1995. Theoretical form factor, attenuation and scattering tabulation for $Z = 1$–92 from $E = 1$–10 eV to $E = 0.4$–1.0 MeV. J. Phys. Chem. Ref. Data 24, 71–643.

Chantler, C.T., Barnea, Z., Tran, C.Q., Tiller, J., Paterson, D., 1999. Precision X-ray optics for fundamental interactions in atomic physics, resolving discrepancies in the X-ray regime. Opt. Quantum Electron. 31, 495–505.

Chantler, C.T., Tran, C.Q., Paterson, D., Barnea, Z., Cookson, D.J., 2000. Monitoring fluctuations at a synchrotron beamline using matched ion chambers: 1. Modelling, data collection, and deduction of simple measures of association. X-ray Spectrom. 29, 449–458.

Creagh, D.C., Hubbell, J.H., 1987. Problems associated with the measurement of X-ray attenuation coefficients. I. Silicon report on the International Union of Crystallography X-ray attenuation project. Acta Crystallogr. A43, 102–112.

Creagh, D.C., McAuley, W., 1995. X-ray dispersion corrections. In: Wilsons, A.J.C. (Ed.), International Table for X-ray Crystallography, Vol. C, Section 4.2.6. Kluwer Academic Publishers, Dordrecht, pp. 206–222.

Henke, B.L., Gullikson, E.C., Davis, J.C., 1993. X-ray interactions: photoabsorption, scattering, transmission and reflection at $E = 50$–30 000 eV, $Z = 1$–92. At. Data Nucl. Data Tables 54, 181–342.

Kiran Kumar, T., Venkataratnam, S., Venkata Reddy, K., 1996. Comments on theoretical limitations for experimental values of photoeffect cross sections at low energies. Nucl. Instrum. Methods B108, 267–275.

Saloman, E.B., Hubbell, J.H., Scofield, J.H., 1988. X-ray attenuation cross sections for energies 100 eV to 100 keV and Elements $Z = 1$ to $Z = 92$. At. Data Nucl. Data Tables 38, 1–197.

Wang, D., Ding, X., Wang, X., Yang, H., Zhou, H., Shen, X., Zhu, G., 1992. X-ray attenuation coefficients and photoelectric cross sections of Cu and Fe in the range 3 keV to 29 keV. Nucl. Instrum. Methods B71, 241–248.